International Journal of Pharmacology

Int. J. Pharmacol. **2025**; 21(6): 45287
https://doi.org/10.31083/IJP45287

Research Article

The Nuclear Translocation of β-catenin in Schwann Cells Influences the Dose-dependent Inhibitory Effects of Flavopiridol on Peripheral Neurodegenerative Processes: A Morpho-pharmacological Approach

Hyung-Joo Chung[1], Jimin Lee[2], Hiroyuki Konishi[3], Kang-Jae Shin[2], Na Young Jeong[2,*], Junyang Jung[4,5,6,*]

[1]Department of Anesthesiology and Pain Medicine, College of Medicine, Kosin University, 49267 Busan, Republic of Korea
[2]Department of Anatomy and Cell Biology, College of Medicine, Dong-A University, 49201 Busan, Republic of Korea
[3]Division of Neuroanatomy, Department of Neuroscience, Yamaguchi University Graduate School of Medicine, 755-8505 Ube, Japan
[4]Department of Biomedical Science, Graduate School, Kyung Hee University, 02447 Seoul, Republic of Korea
[5]Department of Anatomy and Neurobiology, College of Medicine, Kyung Hee University, 02447 Seoul, Republic of Korea
[6]Department of Precision Medicine, College of Medicine, Kyung Hee University, 02447 Seoul, Republic of Korea
*Correspondence: jnyjjy@dau.ac.kr (Na Young Jeong); jjung@khu.ac.kr (Junyang Jung)
Academic Editor: Mehmet Ozaslan
Submitted: 25 July 2025 Revised: 12 August 2025 Accepted: 19 September 2025 Published: 23 October 2025

Abstract

Background: Flavopiridol (Flavo), a synthetic flavonoid derived from *Dysoxylum binectariferum*, broadly inhibits cyclin-dependent kinases (CDKs) that regulate transcription in proliferative cells. In the peripheral nervous system, Schwann cells exhibit transcriptional changes during peripheral neurodegenerative processes (PNPs), involving c-Jun and Krox20 as key regulators. Additionally, hydrogen sulfide (H_2S) promotes neuroprotection by activating the Wnt/β-catenin pathway, which induces cyclin D1 via β-catenin nuclear translocation. **Methods**: To assess the therapeutic potential of Flavo in the PNPs, we conducted experiments targeting Schwann cell responses both *in vivo* and *ex vivo*. Moreover, we examined changes in transcriptional regulation, focusing on c-Jun and Krox20, and analyzed the effect of Flavo on the H_2S/β-catenin/CDK signaling pathway using Western blot and morphological evaluation of demyelination, axonal degeneration, and Schwann cell proliferation. **Results**: Flavo modulated Schwann cell transcription by shifting the c-Jun/Krox20 balance and significantly suppressed abnormal Schwann cell proliferation. The *in vivo* analysis revealed that Flavo dose-dependently reduced demyelination and axonal degeneration. Mechanistically, Flavo inhibited the H_2S/β-catenin/CDK axis, reducing β-catenin nuclear translocation. **Conclusion**: Our findings suggest that Flavo provides multifaceted protection in peripheral nerves by correcting transcriptional dysregulation and attenuating key pathological features of Schwann cell dysfunction. Administering Flavo, in relation to the H_2S/β-catenin/CDK pathway, may represent a promising therapeutic strategy for peripheral neurodegenerative diseases through multitarget transcriptional modulation.

Keywords: Schwann cells; flavopiridol; peripheral neurodegenerative process; hydrogen sulfide; β-catenin

1. Introduction

Schwann cells are unique glia in the peripheral nervous system (PNS) that function to maintain the myelin sheath around peripheral axons, which causes saltatory conduction. Peripheral neurodegenerative process (PNP) occurs in the PNS under abnormal conditions, such as mechanical or toxic injury, and Schwann cells play roles both degenerating and repairing injured Schwann cells functionally and morphologically [1]. After completing PNP Schwann cells promote regeneration of axons to the destination and remyelinate axons to recover saltatory conduction. Therefore, Schwann cells have an all-round capability to solve whatever occurs in the PNS. However, aberrant PNP, such as diabetes mellitus, induces irreversible PNP and ultimately causes peripheral neurodegenerative diseases, such as peripheral diabetic neuropathy [2]. No pathogenetically targeted treatment has been identified.

Schwann cells, the principal glial components of the PNS, are essential for preserving the structural and functional integrity of myelinated axons by forming and maintaining the myelin sheath that enables saltatory conduction. Under pathophysiological conditions, such as mechanical trauma or chemical insult, Schwann cells are not only implicated in the degeneration of damaged nerves but also initiate regenerative responses by undergoing phenotypic and transcriptional reprogramming. This dual role underscores their intrinsic capacity to mediate both degenerative and reparative processes following peripheral nerve injury [1]. Once Wallerian degeneration is complete, Schwann cells facilitate axonal regrowth and remyelination, thereby restoring conduction velocity and functional connectivity. Owing to this multifaceted responsiveness, Schwann cells serve as central effectors in the orchestration of peripheral nerve homeostasis. However, chronic or systemic disorders, including diabetes mellitus, can disrupt this balance and give

rise to maladaptive or incomplete regenerative programs, resulting in irreversible PNP. Such persistent degeneration is a hallmark of peripheral neurodegenerative pathologies like diabetic peripheral neuropathy, for which no disease-modifying therapies currently exist [2].

During PNP, Schwann cells undergo dynamic transcriptional reprogramming that determines their phenotypic fate. In myelinating Schwann cells, positive regulators such as Krox20, as an alias of early growth response 2 (Egr2), SRY-box transcription factor 10 (Sox10), and Oct6, as an alias of POU class 3 homeobox 1 (POU3F1), activate the expression of myelin-related genes [e.g., myelin protein zero (*Mpz*), peripheral myelin protein 22 (*Pmp22*)], reinforcing a stable myelinating state [3]. Conversely, injury-induced demyelination triggers negative transcriptional regulators, particularly c-Jun, which actively represses Krox20-driven programs and promotes a repair phenotype. c-Jun not only suppresses myelin gene expression but also induces pro-regenerative factors such as glial cell line-derived neurotrophic factor (GDNF) and sonic hedgehog (Shh) [4]. While transient c-Jun activation is essential for effective debris clearance and axon guidance, its sustained expression impedes remyelination. Additionally, during demyelination, aberrant activation of canonical Wnt signaling in Schwann cells leads to stabilization and nuclear translocation of β-catenin [5]. Nuclear β-catenin represses myelin gene expression by antagonizing promyelinating transcription factors such as Krox20, thereby disrupting the myelinating phenotype. Sustained β-catenin activity contributes to Schwann cell dedifferentiation and inhibits remyelination, exacerbating PNP. Therefore, the reciprocal antagonism between positive and negative transcriptional factors, such as Krox20 and c-Jun, defines the transcriptional switch between myelinating and demyelinating states, and its dysregulation is implicated in chronic peripheral neuropathies and failed PNP.

Flavopiridol (Flavo), a synthetic derivative of the natural compound rohitukine derived from *Dysoxylum binectariferum*, functions as a potent cyclin-dependent kinase (CDK) inhibitor known to suppress cyclin D1 expression [6,7]. In our investigation, Flavo demonstrated the most pronounced attenuation of PNP phenotypes *in vivo*, notably reducing both axonal degradation and demyelination. Moreover, Flavo modulated transcriptional activity and effectively inhibited β-catenin nuclear translocation in Schwann cells during PNP. These findings collectively indicate that Flavo may serve as a promising prophylactic agent against peripheral neurodegenerative disorders by targeting the hydrogen sulfide (H_2S)/β-catenin/CDK axis to decelerate or prevent neural deterioration.

2. Materials and Methods

2.1 Reagents

Primary antibodies used in this study included cystathionine γ-lyase (CSE; 1:1000, 12217-1-AP, Proteintech Group Inc., Rosemont, IL, USA), β-catenin (1:1000, #9562, Cell Signaling Technology, Boston, MA, USA), phosphorylated Akt (p-Akt; 1:1000, #9271, Cell Signaling Technology, Boston, MA, USA), phosphorylated ERK1/2 (p-ERK1/2; 1:1000, #9101, Cell Signaling Technology, Boston, MA, USA), cyclin D1 (CCND1; 1:1000, #PA5-119058, Invitrogen, Carlsbad, CA, USA), Krox20 (1:1000, #ab43020, Abcam, Cambridge, MA, USA), c-Jun (1:1000, #558036, BD Biosciences, San Jose, CA, USA), neurofilament (NF; 1:1000, #841001, Biolegend, San Diego, CA, USA), myelin basic protein (MBP; 1:1000. #ab980, Millipore, Burlington, MA, USA) and Sox10 (1:1000, Sc-365692, Santa Cruz Biotechnology, Santa Cruz, CA, USA). Secondary antibodies included Alexa fluor-488 donkey anti-mouse (1:20,000, #A32766, Invitrogen, Carlsbad, CA, USA), alexa fluor-488 donkey anti-rabbit (1:20,000, #A32790, Invitrogen, Carlsbad, CA, USA), alexa fluor-594 donkey anti-mouse (1:20,000, #A10037, Invitrogen, Carlsbad, CA, USA), and alexa fluor-594 donkey anti-rabbit (1:20,000, #A10042, Invitrogen, Carlsbad, CA, USA).

2.2 Animal and In Vivo Protocol

Five-week-old healthy male C57BL/6 mice were procured from Samtako Bio Korea (Osan, Korea) and maintained under standard laboratory conditions (23 $\pm$ 1 °C, 12-hour light/dark cycle) with ad libitum access to food and water. All procedures in the mouse experiments were conducted in accordance with the Kyung Hee University Committee on Animal Research guidelines, with approval, ensuring efforts to minimize both animal suffering and the number of animals used [Protocol number #KHSASP-21-463].

For the *in vivo* peripheral nerve injury model, sciatic nerve axotomy was conducted under sterile conditions, as previously described [8]. Anesthesia was induced via intraperitoneal administration of pentobarbital sodium (35 mg/kg body weight, #P3761, Sigma-Aldrich, St. Louis, MO, USA). Pentobarbital sodium was dissolved in sterile saline to prepare a 50 mg/mL stock solution, filtered through a 0.22 µm syringe filter, and stored at 4 °C protected from light. The dosage was adjusted according to body weight to achieve surgical anesthesia. Following transection, the distal segment of each sciatic nerve was enclosed in a 10-mm blind-ended polyvinyl chloride (PVC) tube filled with gel foam pre-soaked in Flavo and maintained *in situ* for 1 to 4 days. Based on this gross observation, we conducted a pharmacoactivity assessment using an *in vivo* system with various concentrations ranging from 1 mM to 100 mM. On each designated post-operative day, animals were euthanized using CO_2 asphyxiation. Mice were euthanized by gradual exposure to CO_2 at a displacement rate of 20–30% of the chamber volume per minute. The distal nerve segments were collected for further analysis. Intact sciatic nerves from uninjured mice served as controls.

2.3 Ex Vivo Sciatic Nerve Explants

For *ex vivo* experimentation, sciatic nerve explant cultures were established based on a previously reported protocol [9]. In brief, sciatic nerves were aseptically isolated from 5-week-old male C57BL/6 mice using fine iris scissors (Fine Science Tools, Foster City, CA, USA) under sterile surgical conditions. The connective tissue surrounding each nerve was carefully removed in phosphate-buffered saline (PBS, #10010-023, Gibco, Thermo Fisher Scientific, Waltham, MA, USA) under a stereomicroscope to ensure clean isolation. The nerves were then cut into 3–4 segments, each measuring approximately 2–3 mm in length, using the same fine scissors. The dissected nerve pieces were transferred to Dulbecco's Modified Eagle Medium (DMEM; #SH30243.01, HyClone, Logan, UT, USA) supplemented with 10% fetal bovine serum (FBS, #16000-044, Gibco, Thermo Fisher Scientific, Waltham, MA, USA) and 1% penicillin-streptomycin (#15140-063, Gibco, Thermo Fisher Scientific, Waltham, MA, USA). Cultures were maintained with or without Flavo for three days in a humidified incubator at 37 °C and 5% CO_2.

2.4 Immunohistochemistry

Tissue sections and teased nerve fibers were fixed with 4% paraformaldehyde (PFA, #158127, Sigma-Aldrich, St. Louis, MO, USA), rapidly frozen using dry ice, and cryosectioned into 6 µm slices. For immunostaining, the slides were incubated with 10% bovine serum albumin (BSA, #37525, Thermo Fisher Scientific, Waltham, MA, USA) for 1 hour at room temperature to block nonspecific binding sites. Subsequently, primary antibodies were applied and incubated overnight at 4 °C in phosphate-buffered saline (PBS) supplemented with 2% BSA. After thorough PBS washes, sections were exposed to Alexa Fluor 488- or 594-conjugated secondary antibodies for 2 hours at room temperature. Fluorescence imaging was performed using a laser scanning confocal microscope (LSM700, Carl Zeiss, Oberkochen, Germany). For quantitative evaluation, we acquired six randomly selected fields per slide using the confocal microscope (LSM 700, Carl Zeiss, Jena, Germany). Each field was captured as a single focal plane (not z-stack images). The total number of images analyzed per experimental group was 36 images from 6 slides, and all images were processed and quantified using the same parameters to ensure consistency.

2.5 Western Blot

Proteins were extracted and lysed in a buffer containing 2% (#L3771, Sigma-Aldrich, St. Louis, MO, USA) and 1% protease inhibitor cocktail (#11697498001, Roche Molecular Biochemicals, Nutley, NJ, USA). To assess protein integrity, samples were resolved on 10% SDS-polyacrylamide gels and stained with Coomassie Brilliant Blue. Following electrophoretic separation, proteins were transferred onto polyvinylidene difluoride (PVDF) membranes (#10600023, Amersham Biosciences, Buckinghamshire, UK). Membranes were then blocked overnight at 4 °C using 5% non-fat dry milk in Tris-buffered saline containing 0.05% Tween-20 (TBST, #7949, Sigma-Aldrich, St. Louis, MO, USA). Subsequently, membranes were incubated with horseradish peroxidase (HRP)-conjugated secondary antibodies using goat anti-mouse IgG-HRP (#sc-2005), goat anti-rabbit IgG-HRP (#2004) and mouse anti-goat IgG-HRP (#sc-2354) from Santa Cruz Biotechnology (Santa Cruz, CA, USA) for signal detection.

2.6 Morphometric Indices

To assess the morphological extent of PNP, four indices were utilized: strip, ovoid, myelin, and neurofilament (NF) indices. The strip index was defined as the count of black or white transverse bands observed within a 500 µm segment of sciatic nerve explants under a stereoscopic microscope. The ovoid index referred to the number of myelin ovoids identified within a 200 µm region of a single teased nerve fiber using differential interference contrast (DIC) microscopy (ZEN 2.3, Carl Zeiss Microscopy GmbH, Jena, Germany). The myelin index represented the proportion of teased nerve fibers among a total of 100 that retained continuous myelin staining exceeding 50 µm in length. The NF index denoted the number of nerve fibers exhibiting uninterrupted neurofilament-positive axonal segments of at least 100 µm in length, out of 100 fibers analyzed per sample [8].

2.7 Statistical Analysis

All data are presented as mean ± standard error of the mean (SEM). Statistical analyses were performed using SPSS version 21.0 (IBM Corp., Armonk, NY, USA). Comparisons between two groups were evaluated using a two-tailed Student's *t*-test, while differences among multiple groups were assessed by one-way analysis of variance (ANOVA) followed by Bonferroni post hoc testing for multiple comparisons. Each experiment was independently repeated at least four times. A *p*-value less than 0.05 was considered statistically significant.

3. Results

3.1 Flavo Exhibits a Dose-dependent Inhibitory Effect on PNP

During PNP, the transverse stripes (bands of Fontana) in sciatic nerves disappeared on day 3 after nerve injury [8]. With this gross property, we performed a pharmacoactivity using an *in vivo* system and various concentrations (1 mM~100 mM) [8]. Among the concentrations, Flavo associated with the CDK signaling pathway significantly inhibited the disappearance of the transverse stripes in sciatic nerves at 3 and 4 days after axotomy (Fig. 1). A toxic effect of 100 mM of Flavo caused the death of Schwann cells; therefore, the stripe index decreased (Fig. 1, left panel). Thus, we used 10 mM of Flavo for further *in vivo* evaluation.

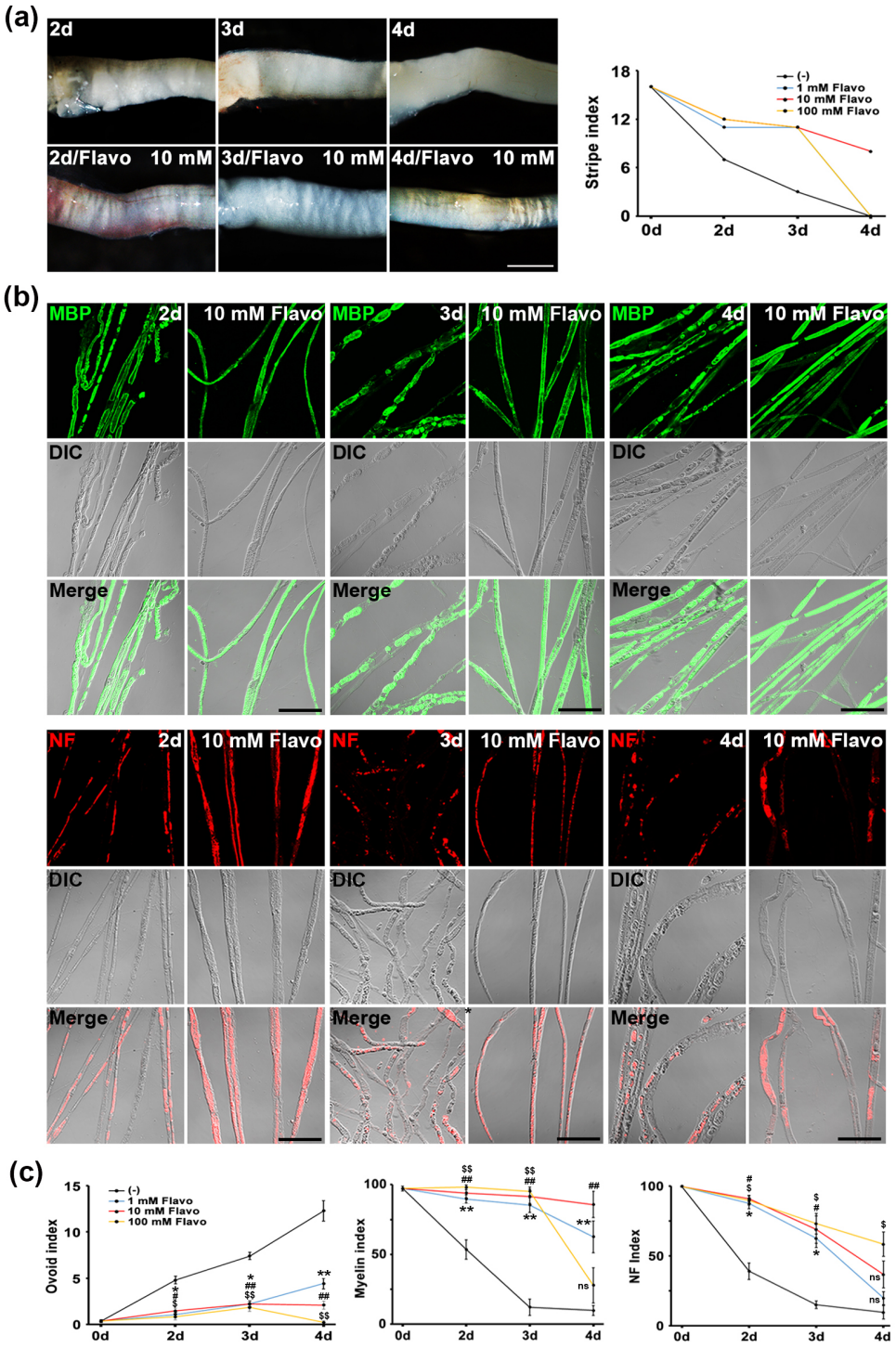

Fig. 1. Flavo inhibits the disappearance of transverse stripes during *in vivo* PNP. (a) Dose-dependent treatment for showing transverse stripe patterns in sciatic nerves (left panel). Scale bar = 600 μm. Quantitative data (right panel) shows the disappearance patterns of transverse stripe under a stereoscope (n = 3 mice). (b) Confocal images show immunolabeling for myelin basic protein as a myelin marker (green; upper panel) and neurofilament as an axon marker (NF, red; lower panel). Scale bar = 100 μm. (c) Ovoid (left panel), myelin (middle panel) and NF (right panel) indices show quantitative degree of *in vivo* PNP (n = 4 mice). $^{*,\ \#\ or\ \$}p < 0.05$ and $^{**,\ \#\#\ or\ \$\$}p < 0.001$. Comparisons between each experimental group (1 mM Flavo, 10 mM Flavo, and 100 mM Flavo) and the control group (Flavo untreated) are indicated as #, $, and *, respectively. ns, not significant. Flavo, flavopiridol; PNP, peripheral neurodegenerative process.

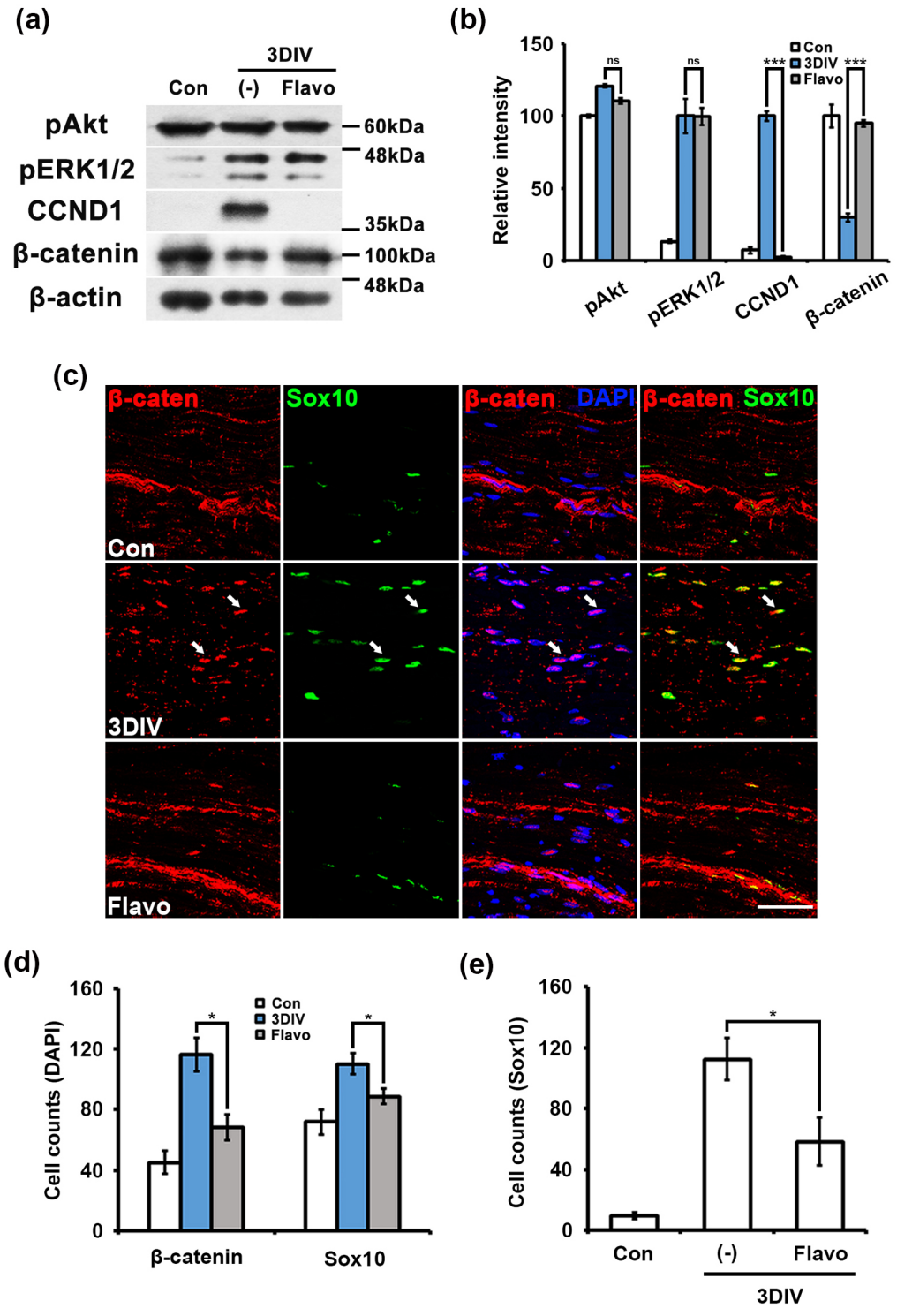

Fig. 2. Flavo inhibits the nuclear translocation of β-catenin in Schwann cells during *ex vivo* PNP. (a) Protein lysates (30 µg) from sciatic explants cultured for 3DIV were analyzed by Western blotting (n = 4 mice). DIV, days *in vitro*; pERK1/2, phosphorylated extracellularregulated kinase 1/2; pAkt, phosphorylated Akt; CCND1, cyclin D1. (b) Quantitative data shows the relative intensities of pAkt, pERK1/2, cyclin D1 and β-catenin in the absence or presence of Flavo (n = 3 mice). $^{***}p < 0.0001$. (c) Confocal images show immunolabeling for β-catenin (β-caten, red). DAPI (blue) and Sox10 (green) are used for nucleus markers. Arrows indicate nuclei double-positive for β-catenin and Sox10. Scale bar = 100 µm. (d) The number of cells was counted with β-catenin immunolabeling out of 200 DAPI-(+) nuclei in teased sciatic nerve fibers as compared with that of the control (n = 4 mice). $^{*}p < 0.05$. (e) The number of cells was counted with β-catenin immunolabeling out of 200 Sox10-(+) nuclei in teased sciatic nerve fibers as compared with that of the control (n = 4 mice). $^{*}p < 0.05$. ns, not significant. Flavo, flavopiridol; PNP, peripheral neurodegenerative process.

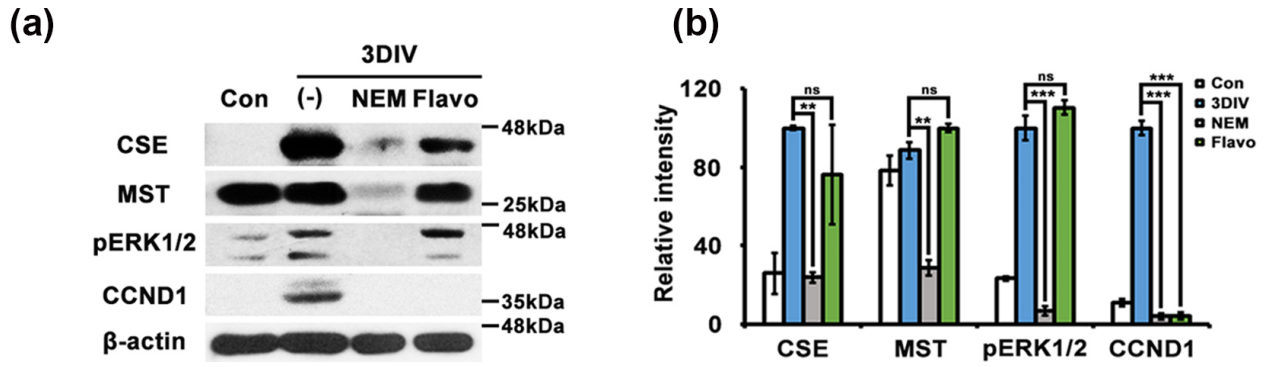

Fig. 3. Flavo fails to suppress the H_2S signaling pathway during *ex vivo* PNP. (a) Protein lysates (30 µg) from sciatic explants cultured for 3DIV were analyzed by Western blotting (n = 4 mice). DIV, days *in vitro*; pERK1/2, phosphorylated extracellularregulated kinase 1/2; CCND1, cyclin D1; cystathionine γ-lyase (CSE); 3-mercaptopyruvate sulfurtransferase (MST). (b) Quantitative data shows the relative intensities of CSE, MST, pERK1/2 and CCND1 in the absence or presence of Flavo (n = 3 mice). $^{**}p < 0.001$ and $^{***}p < 0.0001$. ns, non-significant; PNP, peripheral neurodegenerative process.

3.2 Flavo Plays a Protective Role by Stabilizing Myelin Architecture and Suppressing Axonal Breakdown

PNP is characterized by two primary morphological features: demyelination and axonal degradation. To evaluate whether Flavo can suppress these pathological changes, we conducted immunofluorescent staining using antibodies against myelin basic protein (MBP), a marker of the myelin sheath, and neurofilament (NF), a structural axonal marker, in an established *in vivo* PNP model. In uninjured control sciatic nerves, MBP staining appeared as continuous linear signals along the nerve fibers. By contrast, sciatic nerves examined 3 days post-injury exhibited fragmented MBP signals with irregular boundaries, indicative of Schwann cell demyelination during PNP (Fig. 1b, upper panel). Remarkably, treatment with Flavo preserved the structural integrity of MBP staining at day 3, resembling the intact and linear appearance observed in controls. Following peripheral nerve injury, axonal degradation can result either from intrinsic self-destructive mechanisms or secondary to Schwann cell disintegration [1]. In control samples, NF staining was detected as uninterrupted red fluorescence within the longitudinal axis of nerve fibers (Fig. 1b, lower panel). However, nerves examined 3 days after injury showed a notable increase in interrupted or fragmented NF signals, suggesting significant axonal breakdown. Importantly, Flavo prevented such disruption, maintaining the continuity of NF staining comparable to uninjured nerves.

To quantify these morphological effects, we employed validated morphometric parameters, namely the ovoid (left panel) and myelin (middle panel) indices (reflecting demyelination) and the NF index (reflecting axonal integrity, right panel) [8]. Analysis revealed that Flavo treatment led to a time-dependent reduction in both demyelination and axonal degeneration, as demonstrated by improvements in all three indices (Fig. 1c). Collectively, these findings support the conclusion that Flavo exerts robust protective effects on myelin and axonal structure during *in vivo* PNP.

3.3 Flavo Effectively Regulates H_2S/β-catenin/CDKs in Schwann Cells

Various signaling pathways affect Schwann cell dynamics during PNP. To determine which signaling pathways are involved downstream of H_2S in Schwann cells and whether Flavo regulates these signaling pathways during PNP, we checked the PI3K-Akt [10,11], MAPK [12], and Wnt/β-catenin [5] signaling pathways using western blot analysis. The control and untreated explants exhibited no change of pAkt expression at 3DIV, and Flavo did not inhibit pAkt expression during PNP (Fig. 2a,b). Untreated explants upregulated pERK1/2 at 3 days *in vitro* (3DIV) compared with control explants, which did not express pERK1/2. Flavo did not inhibit the expression of pERK1/2 at 3DIV (Fig. 2a,b). Cyclin D1 is a cell proliferation marker and an effector that represents the pharmacoactivity of Flavo [7,13,14]. Cyclin D1 as a positive control was upregulated at 3DIV in untreated explants and it was suppressed by Flavo at 3DIV (Fig. 2a,b). Thus, we determined that PI3K-Akt and the MAPK/ERK signaling pathways are not regulated by Flavo in Schwann cells during PNP.

The Wnt/β-catenin signaling pathway affects the expression of myelin genes and the maintenance of the myelin structure in Schwann cells [5]. β-catenin was highly expressed in control sciatic nerves, whereas β-catenin expression decreased in untreated 3DIV explants (Fig. 2a,b). The Flavol treatment maintained β-catenin expression similar to that of the control at 3DIV (Fig. 2a,b). Nerve fibers at 3DIV also showed positive β-catenin signals, which overlapped with DAPI staining as a nuclear marker, while Flavo reduced the overlap between the β-catenin and DAPI sig-

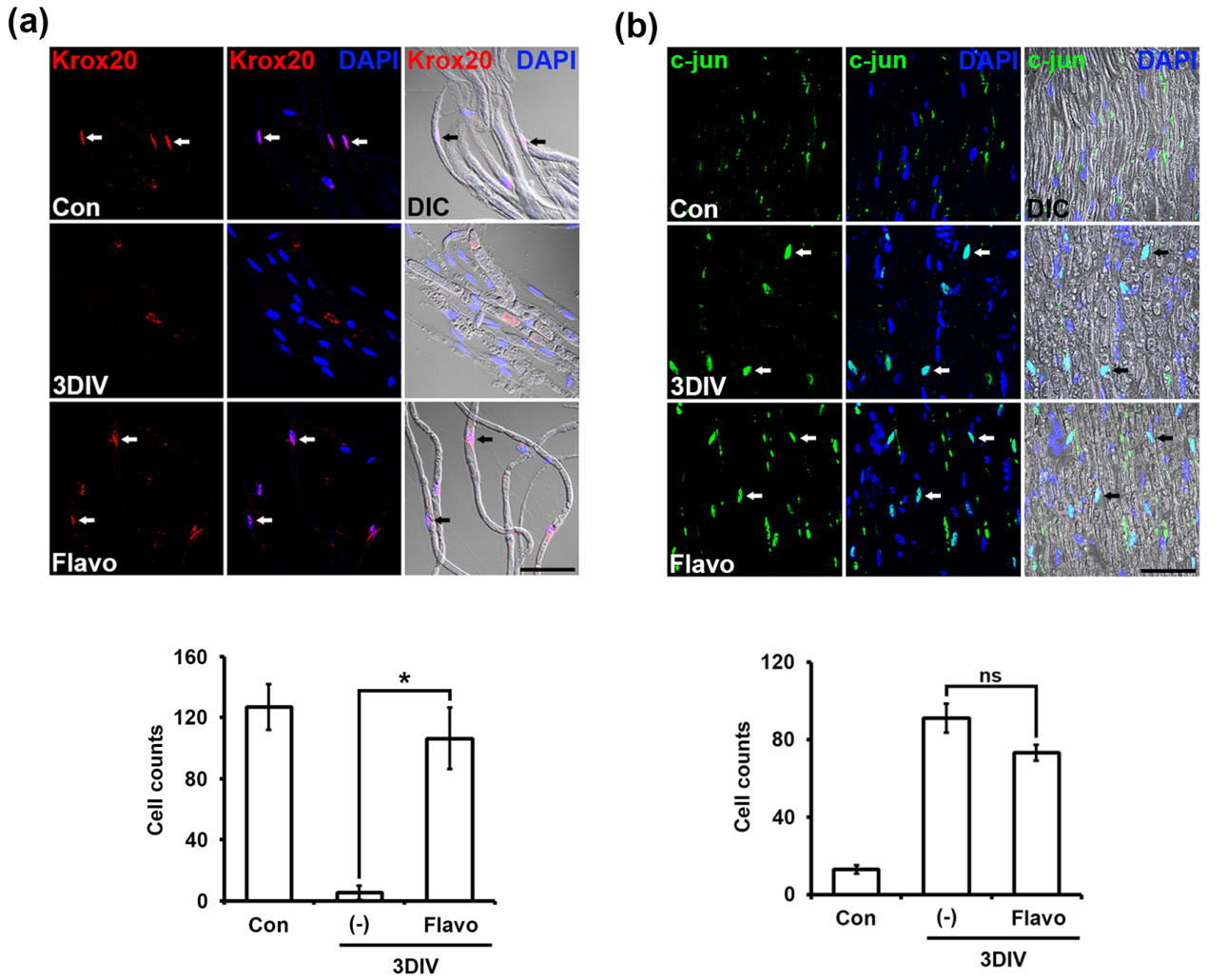

Fig. 4. Flavo controls transcriptional regulation in Schwann cells during *ex vivo* PNP. (a) Confocal images show immunolabeling for Krox20 (red, upper panel). DAPI are used for a nucleus marker (blue). Arrows indicate nuclei double-positive for Krox20 and DAPI. Scale bar = 100 µm. The number of cells was counted with krox20 immunolabeling out of 200 DAPI-(+) nuclei in teased sciatic nerve fibers as compared with that of the control (lower panel, n = 4 mice). $^{*}p < 0.05$. (b) Confocal images show immunolabeling for c-Jun (green, upper panel). DAPI are used for a nucleus marker (blue). Arrows indicate nuclei double-positive for c-Jun and DAPI. Scale bar = 100 µm. The number of cells was counted with c-jun immunolabeling out of 200 DAPI-(+) nuclei in sciatic nerve sections as compared with that of the control (lower panel, n = 4 mice). ns, not significant; DIV, days *in vitro*; Flavo, flavopiridol; PNP, peripheral neurodegenerative process.

nals at 3DIV (Fig. 2c). Quantitative data also indicated that Favo inhibited overlapping β-catenin with positive DAPI or SRY-related HMG-box 10 (Sox10) signals as a marker for nuclei in *ex vivo* culture (Fig. 2d,e). Sox10 is expressed in both myelinating and non-myelinating Schwann cells. Thus, our data suggest that Flavo effectively inhibits the nuclear translocation of β-catenin and affects the Wnt/β-catenin signaling pathway in Schwann cells during PNP.

Additionally, because Flavo is an inhibitor of CDKs, which act downstream of H_2S and induce cell cycle arrest and reduces cyclin D1 [7,15,16], Flavo should not inhibit upstream of CDKs, particularly CSE and 3-mercaptopyruvate sulfurtransferase (MST) as a specific enzyme that produces H_2S in Schwann cells [8]. To determine whether Flavo specifically modulates downstream targets of the H_2S pathway during PNP, we performed western blotting using anti-CSE and anti-MST antibodies in an *ex vivo* model. N-ethylmaleimide (NEM), a specific H_2S inhibitor [8], significantly reduced the expression levels of CSE and MST at 3DIV compared to untreated nerve fibers. In contrast, Flavo did not prevent the reduction in CSE and MST expression in degenerating Schwann cells (Fig. 3a,b), suggesting that CDK signaling acts downstream of the H_2S pathway. Taken together, these findings demonstrate that Flavo effectively suppresses PNP through modulation of the H_2S/β-catenin/CDK signaling pathways.

3.4 Flavo Effectively Controls Transcriptional Regulation Between Krox20 and c-jun in Schwann Cells

Transcriptional regulation in Schwann cells is an essential control tower to exhibit the phenotypes under both normal and degenerating conditions [3]. To assess whether Flavo affects transcriptional regulation during PNP, we checked two transcription factors, such as c-Jun and Krox20, as negative and positive regulators of myelin maintenance, respectively, and performed immunostaining with specific anti- c-Jun and Krox20 antibodies. Krox20 was expressed on the nucleus in Schwann cells from control nerve fibers but did not appear in Schwann cells at 3DIV. Flavo effectively protected the disappearance of Krox20 signaling in Schwann cells at 3DIV (Fig. 4a).

In contrast, c-Jun was not expressed under normal conditions but was highly expressed on the nucleus in untreated Schwann cells at 3DIV (Fig. 4b). Flavo-treated nerve fibers showed no change in c-Jun nuclear expression in Schwann cells at 3DIV compared with that of untreated fibers at 3DIV (Fig. 4b). Taken together, these data indicate that Flavo effectively controls Krox20 expression as a positive transcriptional regulator to maintain myelin structure in Schwann cells in a c-Jun-independent manner.

4. Discussion

4.1 Flavo Regulates PNP via the H_2S/β-catenin/CDK Signaling Pathway

H_2S functions as an antioxidant to reduce oxidative stress in living cells [17]. Thus, most of its downstream molecules are involved in overcoming oxidative stress and a return to normal conditions [17]. In previous studies, H_2S regulated cyclin D1 expression, and cyclin D1 protein levels were regulated by β-catenin [5,15,16,18]. In other words, cyclin D1 expression is induced by the Wnt/β-catenin signaling pathway under increased H_2S, which provides a protective effect against oxidative stress in Schwann cells and activates the boost repair capacity of Schwann cells for effective PNP. In this study, we demonstrated that Flavo did not regulate H_2S production, while Flavo effectively inhibited cyclin D1 expression and nuclear translocation of β-catenin in degenerating Schwann cells (Figs. 2,3). Inhibiting Schwann cell proliferation may prevent the band of Büngner, which is a tunnel that guides the regenerating axon, leading to a delayed or terminated peripheral neurodegenerative process.

4.2 Flavo Effectively Inhibits the Main Schwann Cell Phenotypes During PNP

Peripheral nerves exhibit morphological and biochemical phenotypes, such as demyelination, axonal degradation, transcriptional regulation, Schwann cell transdedifferentiation, and Schwann cell proliferation during PNP. In our study, Flavo significantly inhibited morphologically these phenotypes and arrested PNP (Fig. 1). Schwann cells revert to a dedifferentiated form during PNP, which is also observed in immature Schwann cells during their development [3]. During PNP, axon degradation is regulated both physically and biochemically by Schwann cells [1]. Once PNP begins to progress, dedifferentiating Schwann cells physically dismantle and dissolve axons, thereby inducing axon degradation, while the myelin within Schwann cells undergoes fragmentation mediated by both Schwann cells by itself and macrophages infiltrating from outside of the nerves. Therefore, the effect of Flavo is thought to suppress axon degradation indirectly, rather than directly, by inhibiting CDKs in Schwann cells. In particular, Flavo possesses a potent ability to effectively suppress *in vivo* PNP, suggesting its potential for clinical application (Fig. 1). This suggests that Flavo can effectively penetrate the blood-nerve barrier (BNB), which protects peripheral nerves [19], thereby enabling control of *in vivo* PNP.

Oxidative stress induces c-Jun N-terminal kinase (JNK) activation in several cell types [20] and its inhibitory effect protects c-jun phosphorylation, leading to suppressed c-jun transcriptional activity. In our study, we determined that Flavo did not affect p-c-jun expression in Schwann cells during PNP while Krox20 (Erg2), as a positive regulator of myelin maintenance, was expressed in Flavo-treated Schwann cells at 3DIV (Fig. 4). A previous study reported that P-TEFb *p-Tefb* affects *Krox20* gene expression [21]. Thus, Flavo could canonically affect the transcriptional function of P-TEFb during PNP and subsequently inhibit the decrease in krox20 expression by inactivated P-TEFb, leading to suppressed PNP. In other words, no change in krox20 expression in Flavo-treated Schwann cells could maintain the structure of the myelin and evoke saltatory conduction.

5. Conclusion

Collectively, our findings demonstrate that Flavo exerts a significant inhibitory effect on PNP. Our PNP models revealed that Flavo attenuates hallmark pathological phenotypes, including *in vivo* Schwann cell demyelination and axonal degeneration, as confirmed by morphometric analysis. Mechanistically, Flavo appears to act through modulation of the H_2S/β-catenin/CDK signaling cascade. In general, nerve degeneration and regeneration involve distinct mechanisms, and the pharmacological effect of Flavo is not to regenerate damaged nerves, but rather to preserve the axons and Schwann cell myelin after nerve injury, thereby maintaining their original function. Flavopiridol, a pan-CDK inhibitor, exhibits dose-dependent toxicities that restrict clinical utility. Major adverse effects include diarrhea, neutropenia, fatigue, and hepatotoxicity, arising from broad CDK blockade and off-target transcriptional suppression [22]. Notwithstanding these toxicities, Flavo has been subjected to clinical evaluation across a spectrum of malignancies, including lung cancer and leukemia [6,23]. Repositioning Flavo for peripheral neurodegenerative diseases, as well as the development of novel derivatives, may offer

a promising translational opportunity for addressing these conditions. Thus, we anticipate that this study lays the groundwork for the development of a novel therapeutic approach targeting PNP.

6. Significance Statment

Flavo significantly modulates transcriptional activity in Schwann cells by regulating the complementary roles of c-Jun and Krox20 during PNP. *In vivo*, Flavo dose-dependently attenuated demyelination and axonal degeneration. Mechanistically, Flavo inhibited the H_2S/β-catenin/CDK signaling axis, a critical pathway contributing to aberrant Schwann cell proliferation via β-catenin nuclear translocation and cyclin D1 expression. These findings highlight Flavo's potential as a therapeutic agent for peripheral neurodegenerative diseases through its multi-targeted regulatory effects on Schwann cell dysfunction.

Availability of Data and Materials

The data used to support the findings of this study are available from the corresponding author upon reasonable request.

Author Contributions

Conceptualization, HJC, NYJ and JJ; methodology, HJC, NYJ and JJ; software, JL; validation, HK and K-JS; formal analysis, HJC, NYJ and JJ; investigation, JJ; resources, NYJ; data curation, HJC; writing—original draft preparation HJC, NYJ and JJ; writing—review and editing, HJC, NYJ and JJ; visualization, NYJ; supervision, JJ and NYJ; project administration, JJ; funding acquisition, HJC, NYJ and JJ. All authors contributed to editorial changes in the manuscript. All authors read and approved the final manuscript. All authors have participated sufficiently in the work and agreed to be accountable for all aspects of the work.

Ethics Approval and Consent to Participate

All procedures in the mouse experiments were conducted in accordance with the Kyung Hee University Committee on Animal Research guidelines, with approval, ensuring efforts to minimize both animal suffering and the number of animals used [Protocol number #KHSASP-21-463].

Acknowledgment

We would like to thank Muwoong Kim (Kyung Hee University, Korea) for his valuable help and suggestions.

Funding

This work was supported by Basic Science Research Program through the National Research Foundation of Korea (NRF) funded by the Ministry of Science, ICT and Future Planning, No. 2021R1A2C1004184 (to H-.J.C), No. 2021R1A2C1004133 (to N.Y.J.) and No. 2023R1A2C1003763 (to J.J.).

Conflict of Interest

The authors declare no conflict of interest.

References

[1] Tricaud N, Park HT. Wallerian demyelination: chronicle of a cellular cataclysm. Cellular and Molecular Life Sciences: CMLS. 2017; 74: 4049–4057. https://doi.org/10.1007/s00018-017-2565-2.

[2] Sood A, Kumar B, Singh SK, Prashar P, Gautam A, Gulati M, *et al*. Flavonoids as Potential Therapeutic Agents for the Management of Diabetic Neuropathy. Current Pharmaceutical Design. 2020; 26: 5468–5487. https://doi.org/10.2174/1381612826666200826164322.

[3] Jessen KR, Mirsky R. Negative regulation of myelination: relevance for development, injury, and demyelinating disease. Glia. 2008; 56: 1552–1565. https://doi.org/10.1002/glia.20761.

[4] Arthur-Farraj PJ, Latouche M, Wilton DK, Quintes S, Chabrol E, Banerjee A, *et al*. c-Jun reprograms Schwann cells of injured nerves to generate a repair cell essential for regeneration. Neuron. 2012; 75: 633–647. https://doi.org/10.1016/j.neuron.2012.06.021.

[5] Jacob C, Christen CN, Pereira JA, Somandin C, Baggiolini A, Lötscher P, *et al*. HDAC1 and HDAC2 control the transcriptional program of myelination and the survival of Schwann cells. Nature Neuroscience. 2011; 14: 429–436. https://doi.org/10.1038/nn.2762.

[6] Sedlacek H, Czech J, Naik R, Kaur G, Worland P, Losiewicz M, *et al*. Flavopiridol (L86 8275; NSC 649890), a new kinase inhibitor for tumor therapy. International Journal of Oncology. 1996; 9: 1143–1168. https://doi.org/10.3892/ijo.9.6.1143.

[7] Mihara M, Shintani S, Nakashiro K, Hamakawa H. Flavopiridol, a cyclin dependent kinase (CDK) inhibitor, induces apoptosis by regulating Bcl-x in oral cancer cells. Oral oncology. 2003; 39: 49-55. https://doi.org/10.1016/s1368-8375(02)00019-2.

[8] Park BS, Kim HW, Rhyu IJ, Park C, Yeo SG, Huh Y, *et al*. Hydrogen sulfide is essential for Schwann cell responses to peripheral nerve injury. Journal of Neurochemistry. 2015; 132: 230–242. https://doi.org/10.1111/jnc.12932.

[9] Kim M, Kim H, Kim D, Kim D, Huh Y, Park C, *et al*. Heme Oxygenase 1 in Schwann Cells Regulates Peripheral Nerve Degeneration Against Oxidative Stress. ASN Neuro. 2019; 11: 1759091419838949. https://doi.org/10.1177/1759091419838949.

[10] Taveggia C. Schwann cells-axon interaction in myelination. Current Opinion in Neurobiology. 2016; 39: 24–29. https://doi.org/10.1016/j.conb.2016.03.006.

[11] Figlia G, Norrmén C, Pereira JA, Gerber D, Suter U. Dual function of the PI3K-Akt-mTORC1 axis in myelination of the peripheral nervous system. eLife. 2017; 6: e29241. https://doi.org/10.7554/eLife.29241.

[12] Lee HJ, Shin YK, Park HT. Mitogen Activated Protein Kinase Family Proteins and c-jun Signaling in Injury-induced Schwann Cell Plasticity. Experimental Neurobiology. 2014; 23: 130–137. https://doi.org/10.5607/en.2014.23.2.130.

[13] Jorda R, Hendrychová D, Voller J, Řezníčková E, Gucký T, Kryštof V. How Selective Are Pharmacological Inhibitors of Cell-Cycle-Regulating Cyclin-Dependent Kinases? Journal of Medicinal Chemistry. 2018; 61: 9105–9120. https://doi.org/10.1021/acs.jmedchem.8b00049.

[14] Cicenas J, Kalyan K, Sorokinas A, Jatulyte A, Valiunas D, Kaupinis A, *et al*. Highlights of the Latest Advances in Re-

search on CDK Inhibitors. Cancers. 2014; 6: 2224–2242. https://doi.org/10.3390/cancers6042224.

[15] Zhang J, Ye J, Yuan C, Fu Q, Zhang F, Zhu X, *et al*. Hydrogen sulfide is a regulator of mammary gland development in prepubescent female mice. Molecular Medicine Reports. 2020; 22: 4061–4069. https://doi.org/10.3892/mmr.2020.11462.

[16] Zhang J, Ye J, Yuan C, Fu Q, Zhang F, Zhu X, *et al*. Exogenous H_2 S exerts biphasic effects on porcine mammary epithelial cells proliferation through PI3K/Akt-mTOR signaling pathway. Journal of Cellular Physiology. 2018; 233: 7071–7081. https://doi.org/10.1002/jcp.26630.

[17] Panthi S, Chung HJ, Jung J, Jeong NY. Physiological Importance of Hydrogen Sulfide: Emerging Potent Neuroprotector and Neuromodulator. Oxidative Medicine and Cellular Longevity. 2016; 2016: 9049782. https://doi.org/10.1155/2016/9049782.

[18] Zhang J, Gill AJM, Issacs JD, Atmore B, Johns A, Delbridge LW, *et al*. The Wnt/β-catenin pathway drives increased cyclin D1 levels in lymph node metastasis in papillary thyroid cancer. Human Pathology. 2012; 43: 1044–1050. https://doi.org/10.1016/j.humpath.2011.08.013.

[19] Kanda T. Biology of the blood-nerve barrier and its alteration in immune mediated neuropathies. Journal of Neurology, Neurosurgery, and Psychiatry. 2013; 84: 208–212. https://doi.org/10.1136/jnnp-2012-302312.

[20] Yarza R, Vela S, Solas M, Ramirez MJ. c-Jun N-terminal Kinase (JNK) Signaling as a Therapeutic Target for Alzheimer's Disease. Frontiers in Pharmacology. 2016; 6: 321. https://doi.org/10.3389/fphar.2015.00321.

[21] Fufa TD, Byun JS, Wakano C, Fernandez AG, Pise-Masison CA, Gardner K. The Tax oncogene enhances ELL incorporation into p300 and P-TEFb containing protein complexes to activate transcription. Biochemical and Biophysical Research Communications. 2015; 465: 5–11. https://doi.org/10.1016/j.bbrc.2015.07.072.

[22] Senderowicz AM. Flavopiridol: the first cyclin-dependent kinase inhibitor in human clinical trials. Investigational New Drugs. 1999; 17: 313–320. https://doi.org/10.1023/a:1006353008903.

[23] Zeidner JF, Karp JE. Clinical activity of alvocidib (flavopiridol) in acute myeloid leukemia. Leukemia Research. 2015; 39: 1312–1318. https://doi.org/10.1016/j.leukres.2015.10.010.